Imaging clinical information using dual-source 128-MDCT in two cases of pulmonary atresia and ventricular septal defect

Ristaniah D. Soetikno, MD, and Robby Hermawan, MD

Two cases of PA-VSD were examined by computed tomography angiography (CTA) using dual-source 128-MDCT to reveal the anatomy and morphology of the pulmonary circulation. The first case was diagnosed as PA-VSD type B, while the second case was diagnosed as PA-VSD type A. These cases show that dual-source 128-MDCT can be used to provide clinical information for PA-VSD with the appropriate examination protocols and post-processing techniques.

Introduction

Patients with pulmonary atresia and ventricular septal defect (PA-VSD) need clinical information, specifically the anatomy and morphology of the pulmonary circulation, to determine the surgical approach and overall outcome. Because early treatment can influence the outcome, the information should be acquired as early as possible, while the patient is still young. Capturing meticulous information in a young patient, whose anatomical structures are still small, is a challenging task in imaging. Dual-source 128-MDCT is an alternative, noninvasive imaging modality that can be used for that purpose. Other information, such as coronary and intracardiac abnormalities, can be shown as well.

Case report 1

The first patient was a 19-month-old girl who had delayed growth and development without obvious signs of dyspnea and cyanosis. (The cyanosis was observed only when the patient was crying forcefully.) The patient had never experienced any serious clinical condition that required hospitalization; delayed growth and development was the major problem that led to a thorough clinical examination. The patient had a normal birthweight (2800g), but weight when examined at 19 months was only 5000g. Clinical examination revealed a continuous heart murmur, and chest x-ray showed a "boot-shaped" heart with an upturned cardiac apex and concave pulmonary arterial segment. An echocardiography examination diagnosed the patient with PA-VSD and major aortopulmonary collateral arteries (MAPCAs). The CTA examination was requested for depicting the anatomy and morphology of the pulmonary circulation.

The patient was examined using a dual-source 128-MDCT scanner (Somatom Definition Flash, Siemens Healthcare). Postprocessing of the image data was performed using a Leonardo 3D postprocessing workstation with Syngo software (Siemens Healthcare). Image-reformatting techniques such as curved planar reformation (CPR), maximum-intensity projection (MIP), minimum-intensity projection (MinIP), and volume-rendering technique (VRT) were used to get the information.

The high-density contrast media filled the superior vena cava, right atrium, and right ventricle, as well as the ascending aorta, aortic arch, and descending aorta. But the contrast media density in the left atrium and left ventricle was not as high as in the aorta. Thus, the majority of the aortic flow was from the right ventricle (Fig. 1). There was no stenosis or dilatation of the ascending aorta, aortic arch, or descending aorta. The aortic arch branched to the

The authors are in the Department of Radiology in the Faculty of Medicine at the University of Padjadjaran/Hasan Sadikin Hospital, Bandung, Indonesia. Contact Dr. Soetikno at ristasoetikno@gmail.com.
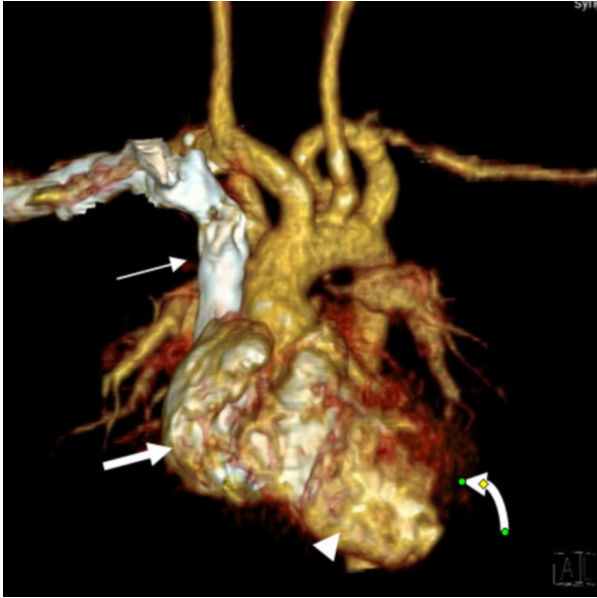
Figure 1. Anterior view VRT of the heart. The high-density contrast media filled the superior vena cava (thin arrow), right atrium (thick arrow), and right ventricle (arrowhead). The aorta was also filled with contrast media, but the left atrium and left ventricle were not filled with the same density contrast media (curved arrow).

brachiocephalic trunk, left common carotid artery, and left subclavian artery.

The proximal pulmonary trunk was not visualized. But high-density contrast media filled the distal pulmonary trunk without clear connection to the right ventricle. The diameter of the distal pulmonary trunk was small (ap-

proximately 0.33 cm). The distal pulmonary trunk divided into the right and left pulmonary arteries, which were also small (diameters, 0.28 cm and 0.26 cm, respectively). Thus, the native pulmonary artery (NPA) was present though small.

The small right pulmonary artery supplied only the superior and middle lobes of the right lung. The right lung had another pulmonary artery supply that came from the systemic circulation. It was larger and located more posteroinferiorly than the previous artery (that came from the distal pulmonary trunk). The larger right pulmonary artery received collateral from the systemic circulation through the right subclavian artery and supplied the inferior lobe of the right lung (Fig. 2). No clear connection was found between the small right pulmonary artery and the large pulmonary artery.

A confluent pulmonary artery connected the small left and right pulmonary arteries. The small right pulmonary artery received its vascularization from the small proximal left pulmonary artery.

Figure 3. Right posterior oblique view VRT of the heart shows the collateral (arrowhead) from the left subclavian artery (thick arrow) to the left pulmonary artery (thin arrow). There is also stenosis (curved arrow) at the collateral artery.

The small proximal left pulmonary artery connected to the distal portion of the left pulmonary artery (which was larger than the proximal part). The larger part of the left pulmonary artery received collateral from the systemic circulation through the left subclavian artery (Fig. 3). The larger part of the left pulmonary artery supplied both the superior and inferior lobes of the left lung.

There was also arterial supply from the descending aorta to the inferior lobes of both lungs. It was difficult to tell whether this was another major aortopulmonary collateral artery or the bronchial artery. There was no patent ductus arteriosus (PDA), and no collateral vascularization from the
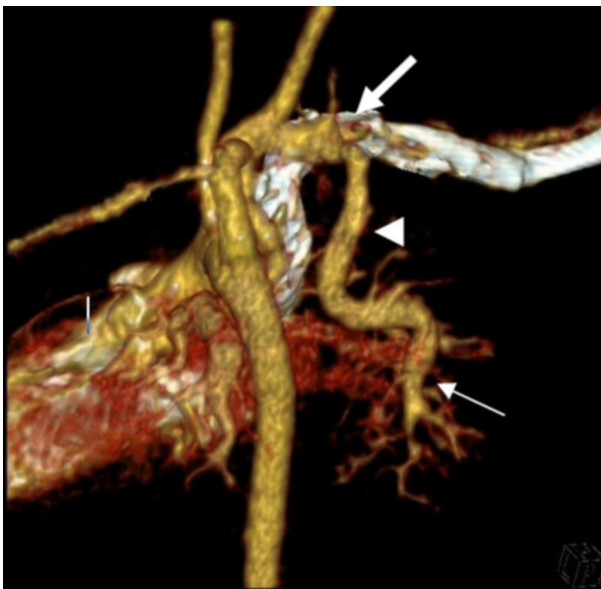

Figure 2. Left posterior oblique view VRT of the heart shows the collateral (arrowhead) from the right subclavian artery (thick arrow) to the right pulmonary artery (thin arrow).

pleura to the lung. Although bilateral pneumonia obscured the pulmonary vascularization, the lung arborization was quite symmetrical.
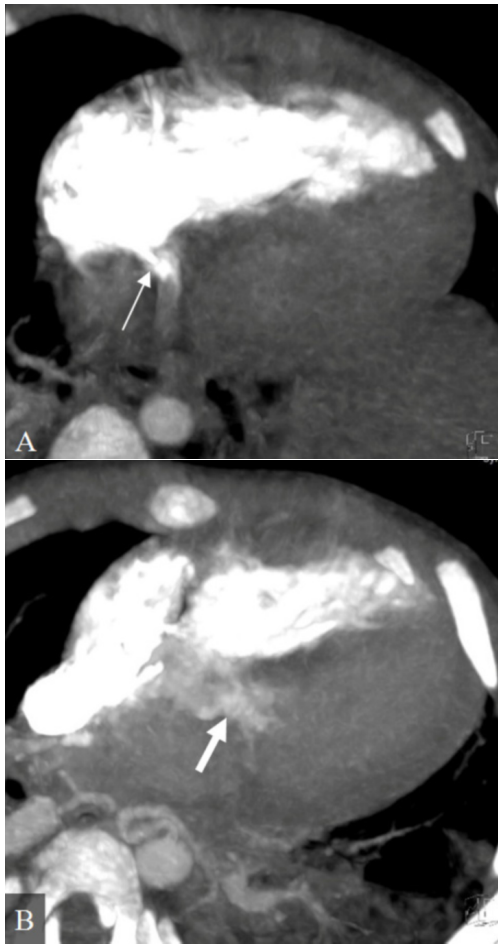

Figure 4. Axial oblique MIP of the heart chamber. (A) Atrial septal defect (thin arrow). (B) Ventricular septal defect (thick arrow).

High-density contrast media had penetrated the interatrial septum (Fig. 4A). This was also true at the interventricular septum (Fig. 4B), so the patient seemed to have atrial and ventricular septal defects.

The right and left coronary arteries originated from the appropriate coronary sinuses. There was clockwise rotation of the aortic root. The course of the coronary arteries was hard to assess.

The trachea was in the midline, without any stenosis or dilatation. The main bronchi were normal. There was no evidence of mass in the anterior, central, or posterior compartments of the mediastinum, nor was there any sign of pleural effusion. Both of the hemidiaphragms were normal. The thoracic skeleton and thoracic soft tissues showed no abnormalities. The liver was on the right side, and the spleen on the left side, so there was no situs anomaly.

Case report 2

The second patient, a 3-month-old boy, had a more severe clinical condition. He was delivered spontaneously, with a low birthweight of 2400g. After delivery, he was hospitalized for eight days because of low birthweight. The patient was cyanotic, especially when he was crying. The clinical examination also revealed a systolic murmur. leading to a suspicion of congenital heart disease. After eight days, the patient was improved and discharged from the hospital. The patient's parents were advised to have a routine clinical evaluation for their child, but they had never come back to the hospital for this. When the patient came back to the hospital at 3 months, he had symptoms of dyspnea, cough, and fever, and his weight was only 3400g. Chest x-ray examination showed heart enlargement and bilateral bronchopneumonia. The patient was diagnosed with PA-VSD by echocardiography. The CTA examination was requested to depict the anatomy and morphology of the pulmonary circulation.
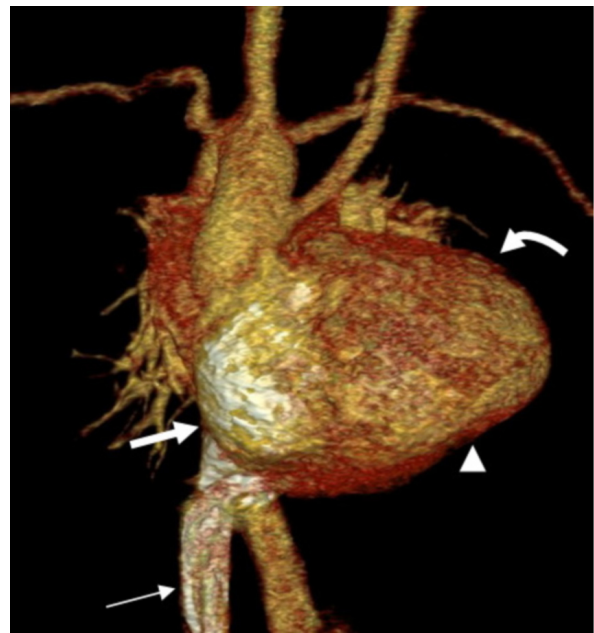

Figure 5. Anterior view VRT of the heart. The high-density contrast media fills the inferior vena cava (thin arrow), right atrium (thick arrow), and right ventricle (arrowhead). The aorta is also filled with contrast media, but the left atrium and left ventricle are not filled with the same density contrast media (curved arrow).

The patient was examined using a dual-source 128-MDCT scanner (Somatom Definition Flash, Siemens Healthcare). The postprocessing techniques of the image data were similar to those for the first patient.

High-density contrast media filled the inferior vena cava, right atrium, and right ventricle (Fig. 5). There was a right-sided aortic arch and overriding of the aorta to the right ventricle (Fig. 6). There was no stenosis or dilatation at the ascending aorta, aortic arch, or descending aorta.
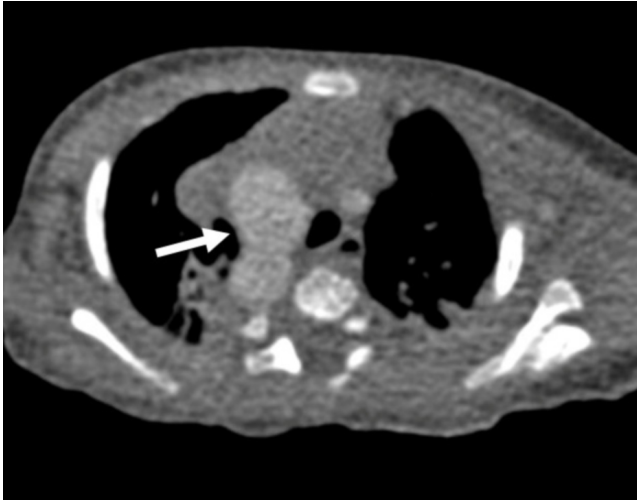
Figure 6. Axial MPR shows the right-sided aortic arch (thick arrow).

There was a PDA with a diameter of 0.2 cm (Fig. 7). The right-sided aortic arch branched to the left common carotid artery, right common carotid artery, right subclavian artery, and aberrant left subclavian artery (Fig. 8). The proximal pulmonary trunk was not visualized. But high-density contrast media filled the distal pulmonary trunk without clear connection to the right ventricle. The diameter of the distal pulmonary trunk was 0.77 cm. The distal pulmonary trunk divided into the right and left pulmonary arteries, with diameters of 0.70 cm and 0.55 cm, respectively. The McGoon ratio was 1.84.
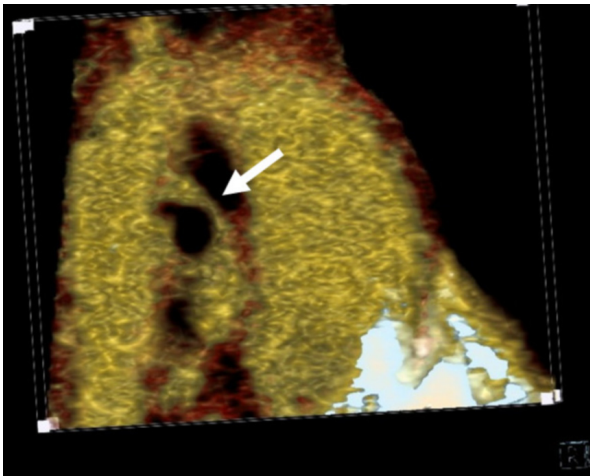

Figure 7. Lateral oblique view VRT of the heart with some cropping. The PDA (thick arrow) is clearly seen in this view.

The right pulmonary artery supplied the superior, middle, and inferior lobes of the right lung. The left pulmonary artery supplied the superior and inferior lobes of the left lung. There was no systemic collateral artery supplying the lung, nor any collateral vascularization from the pleura to

the lung. The lung arborization was quite symmetrical. The patient also had atrial and ventricular septal defects. The coronary arteries were hard to assess. The superior and inferior vena cavas were located at the right side of the spine.
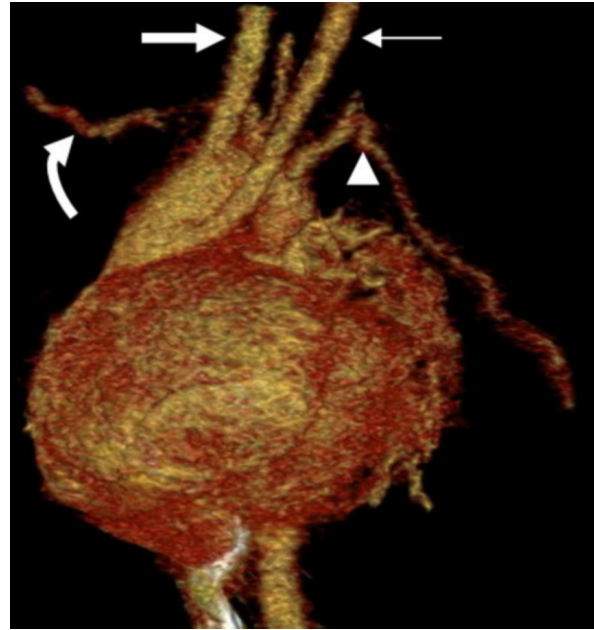

Figure 8. Left anterior oblique view VRT of the heart shows the aberrant left subclavian artery (arrowhead), left common carotid artery (thin arrow), right common carotid artery (thick arrow), and right subclavian artery (curved arrow).

The trachea was in the midline, with no stenosis or dilatation. The main bronchi appeared normal. There was no evidence of mass in the anterior, central, or posterior compartments of the mediastinum, nor any sign of pleural effusion. Both of the hemidiaphragms were normal. The thoracic skeleton and soft tissues showed no abnormalities. The liver was on the right side and the spleen was on the left side, so there was no situs anomaly. There were consolidations with air bronchogram in both of the lungs.

Discussion

Congenital heart disease (CHD) is a structural anomaly of the heart or great vessels that is present at birth. This is the most common single group of congenital abnormalities. The incidence of CHD varies from about 4 to 50 of 1,000 live births (1). A recent Centers for Disease Control and Prevention (CDC) study found that CHD was the main cause of death for 27,960 individuals residing in the United States from 1999 through 2006. Nearly half of these deaths occurred during infancy (2). One of the most dramatic events in pediatrics over the past three decades has been the development of surgical techniques that provide the chance of cure for some children who have CHD and dramatic improvements in quality of life (3).

Pulmonary atresia with ventricular septal defect is a group of congenital heart diseases in which there is lack of continuity between the pulmonary arteries and ventricle; it is associated with ventricular septal defect (4). Pulmonary atresia with ventricular septal defect constitutes 2.5 to 3.4% of all CHD (5). Undiagnosed and untreated PA-VSD can cause complications such as congestive heart failure, erythrocytosis, infective endocarditis, brain abscess, delayed growth and puberty, arrhythmias, and even sudden death (5).

PA-VSD can be classified into three types based on the characterization of the pulmonary circulation (6). In type A, only NPA is supplied by the PDA. In type B, pulmonary blood flow is provided by both NPA and MAPCAs. Type C has only MAPCAs—no NPA (6). This classification has been proposed to guide the surgical approach, although there is always some modification in the management because of the variety of pulmonary blood supply in the PA-VSD.

Providing meticulous information to guide the surgical approach while the patient is still young is a challenging task. Ideally, the imaging modality should depict the pulmonary arteries, other sources of pulmonary blood supply or MAPCAs, the PDA, pleural pulmonary collaterals, bronchial arteries, lung arborization, aortic anomalies, coronary and intracardiac abnormalities, the pulmonary and systemic venous system, and situs anomalies (7). The anatomy and morphology of the pulmonary circulation are the most important pieces of information in determining the treatment of PA-VSD.

Echocardiography is a key diagnostic modality that can assess the anatomy of the central pulmonary artery in infants with PA-VSD, but it does not provide the surgeon with a precise anatomic roadmap (7). Echocardiography is also an operator-dependent modality that is more appropriate to delineate intracardiac abnormalities than extracardiac vascular structures (8).

Catheter angiography is an invasive technique with several disadvantages, such as long sedation time, long procedure time, and complications from arterial puncture (7). Cardiac magnetic resonance imaging (MRI) also has the same problems, since it necessitates long sedation and anesthesia in the closed MRI environment (7). The spatial resolution of MRI is also lower than that of CT, which can be a significant drawback for visualization of small anatomical structures (9).

Dual-source 128-MDCT, with its high temporal and spatial resolution, is an alternative noninvasive imaging modality that can be used to gather clinically related information in the PA-VSD. The anatomy and morphology of the pulmonary circulation can be depicted, as shown in these two cases. In the first case, the MAPCAs were depicted clearly from each subclavian artery to the right and left pulmonary arteries. The small native confluent pulmonary artery was also shown. The PA-VSD in the second case did not have any MAPCAs, but the PDA could be shown from the aorta to the NPA. In conclusion, from the CTA examination, the first case could be diagnosed as PA-VSD type B, while the second case could be diagnosed as PA-VSD type A.

The information gathered not only describes the type of the PA-VSD but also can provide the anatomic roadmap for the surgeon. The three-dimensional VRT technique can demonstrate the shapes and the spatial relationships between the aorta, pulmonary arteries, MAPCAs, PDA, and other anomalous vessels. This is useful particularly in complex cases such as the first case. The aberrant left subclavian artery in the second case was also depicted more clearly with three-dimensional VRT (see Fig. 8, above).

The preoperative evaluation of pulmonary artery size adequacy is also important, because it determines the surgical outcome (9). The McGoon ratio, a pulmonary artery index, has been developed for that purpose. This ratio is calculated by dividing the sum of the diameters of right pulmonary artery (at the level where they cross the lateral margin of the vertebral column and left pulmonary artery just proximal to its upper lobe branch) by the aortic diameter at the level above the diaphragm. A ratio above 1.2 is associated with acceptable postoperative right-ventricle systolic pressure (9). A ratio below 0.8 is deemed inadequate for complete repair of PA-VSD (9). Although the McGoon ratio was originally calculated with angiography, the second case showed that this ratio can also be calculated with CTA examination (Fig. 9). The McGoon ratio in the first case was not calculated because the NPA was too small.
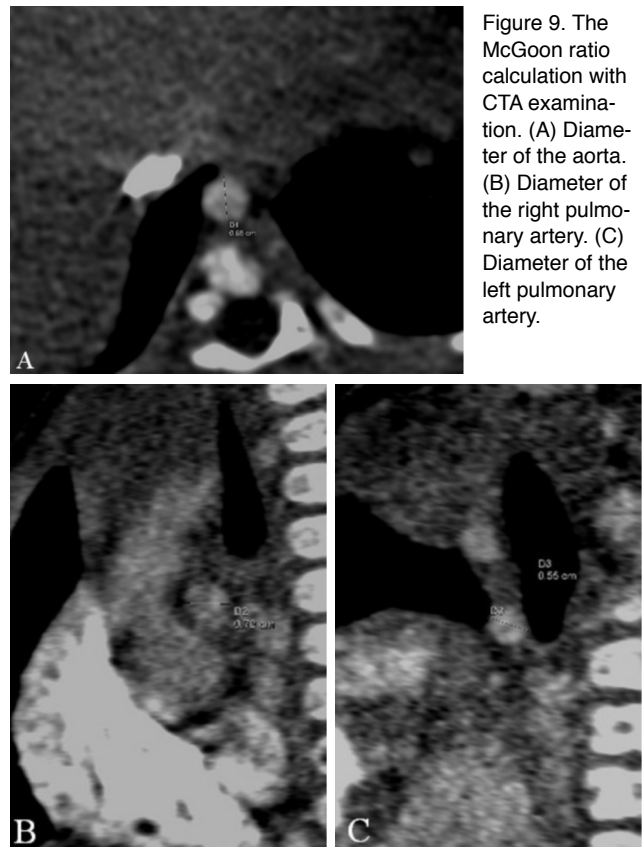

Figure 9. The McGoon ratio calculation with CTA examination. (A) Diameter of the aorta. (B) Diameter of the right pulmonary artery. (C) Diameter of the left pulmonary artery.

Lung arborization can also be assessed, although in these two cases, both patients also had pneumonia that rather obscured the arborization assessment. Although echocardiography is better in delineating intracardiac abnormalities such as atrial septal defect and ventricular septal defect, these two cases show that the septal defects can also be detected by dual-source 128-MDCT.

Coronary anomaly detection in non-ECG gated MDCT is limited to the origin of the major coronary arteries, as was shown in the first case. In the second case, even the origin of the coronary arteries was difficult to identify, probably because the second patient was much younger than the first. There were also differences in the examination protocols; the second case did not use the optimal contrast media flow rate (which will be discussed later).

These two cases show that dual-source 128-MDCT can also depict the systemic venous system, although complete assessment requires two phases (arterial and venous), such as the examination in the second case. The first case was scanned only in the arterial phase, so the inferior vena cava could not be depicted, because the contrast media was injected from the upper extremity. The pulmonary venous system was rather difficult to assess, because both patients had pneumonia that obscured the pulmonary veins (whose density is less than that of the pulmonary artery).

Other clinically related information such as situs anomalies, trachea, and the pulmonary parenchyma can also be assessed with dual-source 128-MDCT, as shown in these two cases (using the soft-tissue window and lung window).

The protocols of the examination are key to achieving optimal results. The examination protocols of both cases were already mentioned previously. The first issue in the scanning protocols is the use of ECG-gated technique. In both of the examinations, this was not used because it was not possible to make the patient hold a breath. Respiratory artifacts greatly degrade images, and such artifacts are substantial with ECG-gated acquisition (7, 9). The heart rates of the patients were also high—124 bpm for the first patient, and 157 bpm for the second. High heart rate makes it difficult to get adequate high-resolution images (7). The radiation dose is also higher than that of non-ECG-gated thoracic CT, because only a part of the dose is used for creating images (9).

The principle of "going as fast as possible" allows good image quality because it minimizes respiratory artifacts (9). With dual-source 128-MDCT Flash Spiral scan, which offers improved temporal resolution compared to the single-source MDCT, this principle can be properly applied with a high pitch scan (10). The scan times for both examinations were 0.51 sec and 0.5 sec, respectively. Although the pitch of both examinations was 3, with dual-source CT scan the real pitch value was 1.5, so there was not too much gap between the slices. Dual-source 128-MDCT Flash Spiral scan also uses a high-pitch technique that reduces the radiation dose (11), as does the reduction of scan repetition due to patient motion.

The second issue is the location and size of the intravenous catheter used for injecting the contrast media. The

preferable intravenous access is a leg vein, to avoid streak artifacts from high-density contrast media in the upper limb veins. An appropriate cannula size (20–22-gauge) should be selected to achieve a high rate of contrast media injection (7). But in reality, radiologists often do not have a choice in determining the location and the size of the intravenous catheter. The patient frequently comes into the examination room with a catheter already placed. Changing the location or the size of the catheter is impractical and sometimes impossible, as happened in the second case. That patient arrived with a small intravenous catheter (26-gauge) located in the antecubital vein. The flow into the catheter was not too good. It was decided to change the catheter to a bigger size and to move it to a leg vein. After almost an hour, the only possible catheter size that could be inserted was a 26-gauge and, because of the delay, the patient was hypothermic, so the examination was postponed to the next day. On the next day, it was decided to inject the contrast media using the available catheter access, but for the safety of the patient, the flow rate had to be reduced to 0.8 mL/s, which was not the optimal rate for a CTA examination. Fortunately, the examination result was good enough to be interpreted as shown in the previous images, although much postprocessing work was needed.

So, the tradeoff in selecting the location and the size of intravenous catheter is between obtaining high-quality images with additional measures to optimize intravenous access—and obtaining lower-quality images without additional manipulation to the already placed catheter. The maximum flow rate for each intravenous catheter size should be maintained for patient safety (12), but keep in mind that the minimum flow rate of 1–1.5 ml/s (with 300–350 mgI/mL contrast media) is necessary for a good-quality CTA result (7, 13).

The first case also shows the impact of inappropriate location of catheter insertion. Although we knew that the appropriate location for the intravenous access is a leg vein, we did not change the already placed intravenous catheter in the antecubital vein because of the practical aspect. The right proximal pulmonary artery that connected to the NPA seems to be cut off from the distal part that supplies the superior lobe of the right lung (Fig. 10). A closer look showed that the separation derived from the artifact caused by high-density contrast media.

In cardiac CT examination of an adult patient, a saline chaser decreases artifact from contrast media and reduces the total amount of contrast media injected (14). Even when a saline chaser is used in infants and neonates, however, the artifact from contrast media is hard to avoid, as shown in these two cases; the chaser serves only to reduce the amount of contrast media needed for CT angiography (7). A longer delay can reduce the artifact, but it adds the risk of missing the optimum high-contrast media density in the pulmonary artery, and the high-contrast media density helps to intepret the result. In both cases, the conclusion that the majority of the aortic flow had come from the right ventricle was made because the high-contrast media density had already filled the aorta, while the left atrium
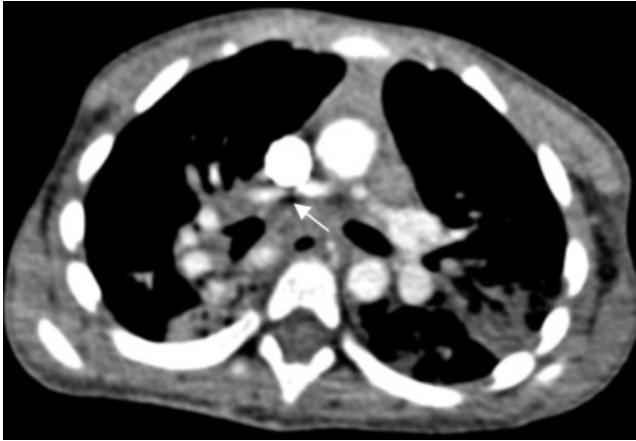
Figure 10. The right proximal pulmonary artery seemed to be cut off from the distal part. Slice-by-slice image analysis shows that this cut off was because of the artifact (thin arrow).

and ventricle were not filled with the same density of contrast media. The septal defects were also easily detected because the contrast media density in the right-sided and left-sided chambers were different. The flow of high-contrast media density from the right chamber to the left chamber was easily seen and could be interpreted as a septal defect.

The delay can be set using a bolus-tracking technique, but these two cases did not use it. The risk of misplacing the region of interest (ROI) is our concern in using the bolus-tracking technique, especially in congenital heart disease patients, where the anatomic structure of the heart is hard to predict. The delay of scanning was determined to be between 10 and 15 seconds, depending on the site of injection (9).

Postprocessing techniques also play a vital role in the evaluation of the image data. 3D imaging with VRT is the first-line approach for interpretation, due to the complexity and spatial variety of the anatomical structures (9), but MPR and MIP are still used to confirm the vascular condition. 3D images are also preferred by the clinicians. Curved planar reformatting is helpful when evaluating curved structures such as the pulmonary arteries and MAPCAs for any stenosis or dilatation (7).

References

1. Hoffman JI, Kaplan S. The incidence of congenital heart disease. *J Am Coll Cardiol*. 2002 Jun;39(12):1890–900. [PubMed]
2. Gilboa SM, Salemi JL, Nembhard WN, Fixler DE, Correa A. Mortality resulting from congenital heart disease among children and adults in the United States, 1996 to 2006. *Circulation*. 2010 Nov; 122(22): 2254-63. [PubMed]
3. Morris CD. Epidemiology of congenital heart disease. In: Crawford MH, DiMarco JP, Paulus WJ, eds. *Cardiology*. Philadelphia: Elsevier Ltd, 2010:1379–91.
4. O'Leary PW, Edwards WD, Julsrud PR, Puga FJ. Pulmonary atresia and ventricular septal defect. In: Allen HD, Driscoll DJ, Shaddy RE, Feltes TF, eds. *Moss and Adam's heart disease in infants, children, and adolescents*. Baltimore, MD: Lippincott Williams & Wilkins; 2008:878–88.
5. Rodriguez-Cruz E, Aggarwal S, Delius RE. Pulmonary atresia with ventricular septal defect. *Medscape [Internet]*. 2012 Apr 17 [cited 2013 Sep 23]. Available from: http://emedicine.medscape.com/article/905119-overview
6. Tchervenkov CI, Roy, N. Congenital Heart Surgery Nomenclature and Database Project: Pulmonary atresia-ventricular septal defect. *Ann Thorac Surg*. 2000 Apr;69[4 suppl]:S97–105. [PubMed]
7. Rajeshkannan R, Moorthy S, Sreekumar KP, Ramachandran PV, Kumar RK, Remadevi KS. Role of 64-MDCT in evaluation of pulmonary atresia with ventricular septal defect. *AJR Am J Roentgenol*. 2010 Jan;194(1):110–8. [PubMed]
8. Balaguru D, Dilawar M. Pulmonary atresia with ventricular septal defect: systematic review. *Heart Views* 2007;2(8):52–61. [cited 2013 Jun 16]. Available from: http://www.heartviews.org/article.asp?issn=1995705X;year=2007;volume=8;issue=2;spage=52;epage=61;aulast=Balaguru
9. Paul JF. Diagnosis of congenital heart disease in adults and children. In: Ohnesorge BM, Flohr TG, Becker CR, Knez A, Reiser MF, eds. *Multi-slice and dual-source CT in cardiac imaging*. Berlin Heidelberg: Springer-Verlag, 2007:258–65.
10. Ohnesorge BM. Future technical developments in cardiac CT. In: Ohnesorge BM, Flohr TG, Becker CR, Knez A, Reiser MF, eds. *Multi-slice and dual-source CT in cardiac imaging*. Berlin Heidelberg: Springer-Verlag, 2007:327–58.
11. Fink C, Krissak R, Henzler T, et al. Radiation dose at coronary ct angiography: second-generation dual-source CT versus single-source 64-MDCT and first generation dual-source CT. *AJR Am J Roentgenol*. 2011 May;196:W550–7. [PubMed]
12. Amaral JG, Traubici J, BenDavid G, Reintamm G, Daneman A. Safety of power injector use in children as measured by incidence of extravasation. *AJR Am J Roentgenol*. 2006 Aug;187:580–3. [PubMed]
13. Siegel MJ. CT angiography: optimizing contrast use in pediatric patients. *Applied Radiology* 2003;12(32):43–9. [cited 2013 Jun 16]. Available from : http://www.appliedradiology.com/Issues/2003/12/Supplements/CT-angiography--Optimizing-contrast-use-in-pediatric-patients.aspx
14. Pannu HK, Flohr TG, Corl FM, Fishman EK. Current concepts in multi-detector row CT evaluation of the coronary arteries: principles, techniques, and anatomy. *Radiographics*. 2003 Oct;23:S111–25. [PubMed]